Adaptive Clarke Transformation for Robust Estimation of Three-Phase Grid Frequency

Md Shamim Reza, Matthew Priestley, Elias Aboutanios and John Fletcher
School of Electrical Engineering and Telecommunications
University of New South Wales, Sydney, NSW 2052, Australia
Email: md_shamim.reza@unsw.edu.au, m.priestley@unsw.edu.au, elias@ieee.org, john.fletcher@unsw.edu.au

***Abstract*—A grid-synchronization algorithm for grid-tie inverters must be precise, accurate, robust to noise and harmonic distortion and fast to react to grid voltage disturbances to facilitate stable operation in a modern distribution grid network. Unlike traditional synchronization algorithms such as the phase-locked loop (PLL), the harmonic version of the Aboutanios and Mulgrew (HAM) algorithm performs well in all these characteristics. However, both the three-phase HAM estimator and three single-phase HAM estimators generate some small estimation error during unbalanced grid voltage conditions. This paper proposes a method that combines the adaptive Clarke transform (ACT) with the HAM estimator to reduce this error and cause convergence to the Cramèr Rao Lower Bound in noisy environments under both balanced and unbalanced conditions. Simulated results confirm that the proposed method generates improved performance when compared to several similar competing estimators.**

***Index Terms*—adaptive Clarke transform (ACT), Fourier coefficients, fundamental frequency, harmonic version of Aboutanios and Mulgrew (HAM) algorithm, and orthogonal signals.**

I. Introduction

The estimation and tracking of the frequency, amplitude and phase is necessary for various tasks in power systems [1][2]. Several international standards and codes have been established to define the functioning range of the grid frequency, and any device connecting to it must synchronise to the grid voltage to align with these standards [3][4]. Thus, accurate, precise and robust estimation of the fundamental frequency, amplitude and phase is essential for effective, reliable and safe grid operation. Yet, this is still a challenge, particularly in the presence of grid voltage imbalances and harmonic distortion.

Various methods exist for the tracking of frequency in three-phase grids, including the Kalman filter [5], phase-locked loop (PLL) [6], frequency-locked loop [7], complex least mean squares [8], Teager energy operator [9], and digital filter-based algorithm [10]. All these estimation methods require the generation of two orthogonal signals from the three measured grid voltages, which is achieved by the standard Clarke transform (CT). However, the CT fails to yield orthogonal signals under unbalanced voltage conditions [11][12][13][14]. Furthermore, most grid frequency estimation methods require low harmonic distortion to produce accurate estimation. Yet, harmonic distortion is commonly present in grid voltage signals due to nonlinear loads connected to the grid. As a result, the accuracy of frequency estimation may degrade if harmonic distortion is not taken into account. Pre- or in-loop filters are employed to improve the estimation accuracy, but this comes at the expense of a reduced frequency estimation range and a slower response. Therefore, a compromise is demanded between speed and accuracy for tuning the parameters of the techniques.

The presence of harmonics can be handled by parametric estimators, such as MUSIC [15], ESPRIT [16] and the Fourier-based harmonic version of the Aboutanios and Mulgrew (HAM) algorithm [17][18][19]. These algorithms also rely on the CT for generating a complex multi-tone signal for three-phase systems. A weighted least square (WLS) approach that exploits the harmonic structure, can also be combined with the estimators to further improve accuracy [20][21]. However, the improvement due to the WLS approach is observed when the higher order harmonics are relatively large and the signal to noise ratio (SNR) is high.

This paper proposes a robust method that combines an adaptive CT (ACT) with the HAM estimator to track the three-phase grid frequency in the presence of voltage imbalances and distortions. The proposed method can converge to the Cramèr Rao Lower Bound (CRLB) for tracking the fundamental frequency under both balanced and unbalanced conditions as well as harmonic distortion. It enjoys improved performance when compared to the standard CT-based HAM estimator (CT-HAM), averaged three HAM (3-HAM) estimators, and averaged three second-order generalised integrator-based PLLs (3-SOGI-PLL) for three individual single-phase voltage signals.

The remainder of the paper is organised as follows. Section II details the proposed ACT-HAM estimator. Simulated results and comparison with state-of-the-art methods are reported in section III. Finally, conclusions are summarised in Section IV.

II. Proposed ACT-HAM Method

The three-phase grid voltage signals without harmonic distortions can be expressed as

$$\begin{bmatrix} v_a(n) \\ v_b(n) \\ v_c(n) \end{bmatrix} = \begin{bmatrix} A_a \cos(2\pi f n + \theta_a)] \\ A_b \cos(2\pi f n + \theta_b)] \\ A_c \cos(2\pi f n + \theta_c)] \end{bmatrix} + \begin{bmatrix} w_a(n) \\ w_b(n) \\ w_c(n) \end{bmatrix}, \quad (1)$$

where n is the sample index, f the normalised fundamental frequency, and A_p, θ_p and w_p ($p \in \{a, b, c\}$) are the amplitude, initial phase angle and noise, respectively, of phase voltage v_p. The noise signals are assumed as independent identically distributed (iid) Gaussian with zero mean and variance $\sigma^2/2$. Note that the three-phase system is balanced when $A_a = A_b = A_c$ and $\theta_a = \theta_b + 2\pi/3 = \theta_c - 2\pi/3$; otherwise it is unbalanced.

979-8-3503-3959-8/23/$31.00

A. Adaptive Clarke Transform (ACT)

The ACT is able to generate orthogonal voltage signals under both balanced and unbalanced conditions in three-phase voltage systems [11]. Voltage imbalances can manifest as unequal amplitudes and/or phase displacements that are not 120° due to asymmetrical grid faults or unbalanced loading. The ACT can be expressed by the following novel transformation

$$\begin{bmatrix} v_\alpha(n) \\ v_\beta(n) \end{bmatrix} = \mathbf{G} \begin{bmatrix} v_a(n) \\ v_b(n) \\ v_c(n) \end{bmatrix} = \begin{bmatrix} \cos(2\pi fn) \\ \sin(2\pi fn) \end{bmatrix} + \begin{bmatrix} w_\alpha(n) \\ w_\beta(n) \end{bmatrix}, \quad (2)$$

where $\mathbf{G} = [\boldsymbol{\alpha}\ \boldsymbol{\beta}]^T$, $\boldsymbol{\alpha} = [\alpha_a\ \alpha_b\ \alpha_c]$, $\boldsymbol{\beta} = [\beta_a\ \beta_b\ \beta_c]$, T denotes transpose operation and the α_p and β_p $(p = a, b, c)$ are

$$\begin{aligned} \alpha_p &= \frac{A_p}{A_T^2} \sum_{i\in\{a,b,c\}, i\neq p} A_i^2 \sin(\theta_i - \theta_p)\sin(\theta_i) \\ \beta_p &= \frac{A_p}{A_T^2} \sum_{i\in\{a,b,c\}, i\neq p} A_i^2 \sin(\theta_i - \theta_p)\cos(\theta_i) \\ A_T^2 &= \frac{1}{2} \sum_{i\in\{a,b,c\}} A_i^2 \sum_{j\in\{a,b,c\}, j\neq i} A_j^2 \sin^2(\theta_i - \theta_j) \end{aligned}$$

Here, $\mathbf{G}$ is the ACT matrix, and w_α and w_β the noise components of the generated orthogonal signals. The above coefficients of the ACT matrix are derived by the steps reported in [11]. They are obtained by minimising the output noise variance whilst maintaining the unity amplitude of the output signals, thus maximising the output SNR. When only amplitude imbalance is present, the ACT is identical to the form reported in [11]. Furthermore, the ACT reduces to the standard CT when all amplitudes are equal (i.e. $A_a = A_b = A_c = 1$). The voltage signals, obtained by the ACT shown in (2), can be combined to give a complex exponential signal

$$v_{\alpha\beta}(n) = v_\alpha(n) + jv_\beta(n) = e^{j2\pi fn} + w_{\alpha\beta}(n), \quad (3)$$

where $w_{\alpha\beta}$ is the complex Gaussian noise with zero mean and variance that is shown to be [11]

$$\sigma_{\alpha\beta}^2 = (\alpha_a^2 + \alpha_b^2 + \alpha_c^2 + \beta_a^2 + \beta_b^2 + \beta_c^2)\sigma^2/2. \quad (4)$$

If the three-phase voltage signals contain K harmonics with orders $k = 1, 2, 3, \ldots, K$, then the output voltage becomes

$$v_{\alpha\beta}(n) = \sum_{k=1}^{K} (C_k e^{j2\pi kfn} + C_{-k} e^{-j2\pi kfn}) + w_{\alpha\beta}(n), \quad (5)$$

where

$$\begin{aligned} C_k &= [A_{ak} e^{j\theta_{ak}} \zeta_a + A_{bk} e^{j\theta_{bk}} \zeta_b + A_{ck} e^{j\theta_{ck}} \zeta_c]/2 \\ C_{-k} &= [A_{ak} e^{-j\theta_{ak}} \zeta_a + A_{bk} e^{-j\theta_{bk}} \zeta_b + A_{ck} e^{-j\theta_{ck}} \zeta_c]/2. \end{aligned}$$

Here, $C_1 = 1$, $C_{-1} = 0$, C_k and C_{-k} are the complex amplitudes of the exponentials corresponding to the positive and negative frequency components of the k^{th} harmonic, $\zeta_p = \alpha_p + j\beta_p$, and A_{pk} and θ_{pk} $(p = a, b, c)$ are respectively the amplitudes and initial phase angles of the k^{th} harmonic of phase p. The complex signal in (5) can be used to estimate the fundamental frequency using the HAM estimator presented below.

B. HAM Estimator

The HAM estimator comprises two steps: a coarse search and a refinement step using interpolation on Fourier coefficients. Given N samples of $v_{\alpha\beta}$, the coarse stage yields an initial estimate of the fundamental frequency as the frequency bin corresponding to the maximum magnitude of the FFT of $v_{\alpha\beta}(n)$, $n = 0, 1, \ldots, N-1$. That is,

$$\hat{f}_0 = \frac{\hat{m}_0}{N}, \quad (6)$$

where $\hat{m}_0 = \arg\max_m |V(m)|^2$, $(\hat{\ })$ denotes the estimate, and V is the N point FFT of $v_{\alpha\beta}$. The initial frequency estimate in (6), is refined using two coefficients ($V_{\pm 0.5}$) of the DFT, which are adjacent to the frequency $\hat{f}_0$. The spectral leakage affected DFT coefficients ($\tilde{V}_{\pm 0.5}$) at frequencies $\hat{f}_0 \pm 0.5/N$ are given by

$$\begin{aligned} \tilde{V}_{\pm 0.5} &= \sum_{n=0}^{N-1} v_{\alpha\beta}(n) e^{-j2\pi(\hat{f}_0 \pm 0.5/N)n} \\ &= V_{\pm 0.5} + \sum_{k=2}^{K} (V_{\pm 0.5,k} + V_{\pm 0.5,-k}) + W_{\pm 0.5}, \end{aligned} \quad (7)$$

where

$$V_{\pm 0.5,k} = C_k \frac{1 + e^{j2\pi N(kf - \hat{f}_0)}}{1 - e^{j2\pi(kf - \hat{f}_0)} e^{\mp j\pi/N}}.$$

The terms $W_{\pm 0.5}$ are the Fourier coefficients of the noise at frequencies $\hat{f}_0 \pm 0.5/N$. In the refinement step, the spectral leakages ($V_{\pm 0.5,k}$ and $V_{\pm 0.5,-k}$) corresponding to the undesired positive (kf) and negative ($-kf$) frequencies of the harmonics are subtracted from the DFT coefficients $\tilde{V}_{\pm 0.5}$ to yield leakage free coefficients ($V_{\pm 0.5}$). Assuming C_k and C_{-k} are known or estimated ($\hat{C}_k$ and $\hat{C}_{-k}$), then the spectral leakage at frequencies $\hat{f}_0 \pm 0.5/N$ can be obtained as

$$\hat{V}_{\pm 0.5,k} = \hat{C}_k \frac{1 + e^{j2\pi N(k-1)\hat{f}_0}}{1 - e^{j2\pi(k-1)\hat{f}_0} e^{\mp j\pi/N}}. \quad (8)$$

The leakage-free Fourier coefficients are then given by

$$\hat{V}_{\pm 0.5} = \tilde{V}_{\pm 0.5} - \sum_{k=2}^{K} (\hat{V}_{\pm 0.5,k} + \hat{V}_{\pm 0.5,-k}). \quad (9)$$

The normalized fundamental frequency is then updated by interpolating on the leakage-free Fourier coefficients, giving

$$\hat{f} = \hat{f}_0 + \frac{\mathrm{Im}\,(\ln(\hat{z}))}{2\pi} \quad (10)$$

where

$$\hat{z} = \left[\cos(\frac{\pi}{N}) - j \frac{\hat{V}_{+0.5} + \hat{V}_{-0.5}}{\hat{V}_{+0.5} - \hat{V}_{-0.5}} \sin(\frac{\pi}{N}) \right]^{-1}.$$

The functions 'Im(z)' and 'ln' are the imaginary part and natural logarithm, respectively. The fundamental frequency estimate (10) is now used to obtain the amplitude and phase angle of each phase voltage as follows. Casting the N samples of each phase voltage signal in vector form, we write

$$\mathbf{v}_p = \mathbf{Z}_{\hat{f}} \mathbf{a}_p + \mathbf{w}_p, \quad (11)$$

TABLE I: Proposed ACT-HAM Method

Given:	N samples of voltages $v_p(n)$, $p = a, b, c$
Initialize:	$\mathbf{G}$=standard CT matrix, $\hat{C}_k = \hat{C}_{-k} = 0$
Coarse Stage:	$\mathbf{v} = \mathbf{G}\mathbf{v}_{abc}$, $\mathbf{v} = [v_\alpha \ v_\beta]^T$, $\mathbf{v}_{abc} = [v_a \ v_b \ v_c]^T$
	$v_{\alpha\beta} = v_\alpha + jv_\beta$
	$V(m)$=FFT$(v_{\alpha\beta})$, $m = 0, 1, ..., N-1$
	$\hat{m}_0$=value of m when $\lvert V(m)\rvert^2$ is maximum
	$\hat{f} = \hat{f}_0 = \hat{m}_0/N$
Refinement:	Iteration starts: $q = 1$ to Q
	$\tilde{V}_{\pm 0.5} = \sum_{n=0}^{N-1} v_{\alpha\beta}(n) e^{-j2\pi(\hat{f} \pm 0.5/N)n}$
	$\hat{V}_{\pm 0.5,k} = \hat{C}_k \frac{1+e^{j2\pi N(k-1)\hat{f}}}{1-e^{j2\pi(k-1)\hat{f}} e^{\mp j\pi/N}}$
	$\hat{V}_{\pm 0.5} = \tilde{V}_{\pm 0.5} - \sum_{k=2}^{K} (\hat{V}_{\pm 0.5,k} + \hat{V}_{\pm 0.5,-k})$
	$\hat{z} = \left[\cos(\frac{\pi}{N}) - j\frac{\hat{V}_{+0.5}+\hat{V}_{-0.5}}{\hat{V}_{+0.5}-\hat{V}_{-0.5}} \sin(\frac{\pi}{N})\right]^{-1}$
	$\hat{f} = \hat{f} + [\mathrm{Im}\,(\ln(\hat{z}))]/2\pi$
	$\hat{\mathbf{a}}_p = \mathbf{Z}_{\hat{f}}^{\#}\mathbf{v}_p$, where $\mathbf{Z}_{\hat{f}}^{\#} = [\mathbf{Z}_{\hat{f}}^H \mathbf{Z}_{\hat{f}}]^{-1}\mathbf{Z}_{\hat{f}}^H$
	Calculate $\hat{A}_{pk}$ & $\hat{\theta}_{pk}$ from $\hat{\mathbf{a}}_p$
	Update $\mathbf{G}$, $\hat{C}_k$ & $\hat{C}_{-k}$
	Update $\mathbf{v}$ & $v_{\alpha\beta}$
Output:	Estimated fundamental frequency=$f_s\hat{f}$

where $\mathbf{v}_p = [v_p(0) \ldots v_p(N-1)]^T$, $\mathbf{Z}_{\hat{f}} = [\mathbf{Z}_{n1} \ \mathbf{Z}_{n1}^* \ldots \mathbf{Z}_{nK} \ Z_{nK}^*]$, $\mathbf{Z}_{nk} = [1 \ e^{j2\pi k\hat{f}1} \ldots e^{j2\pi k\hat{f}(N-1)}]^T$, $\mathbf{a}_p = [a_{p1} \ a_{p1}^* \ldots a_{pK} \ a_{pK}^*]^T$, $a_{pk} = A_{pk}e^{j\theta_{pk}}/2$ and the superscript $*$ represents complex conjugate. Then $\mathbf{a}_p$ can be obtained via least square (LS) as

$$\hat{\mathbf{a}}_p = \mathbf{Z}_{\hat{f}}^{\#}\mathbf{v}_p, \tag{12}$$

where $\mathbf{Z}_{\hat{f}}^{\#} = [\mathbf{Z}_{\hat{f}}^H \mathbf{Z}_{\hat{f}}]^{-1}\mathbf{Z}_{\hat{f}}^H$ and the superscript H denotes Hermitian transpose operation. The amplitude and initial phase angle of the k^{th} harmonic component of each phase voltage signal $(v_p, p = a, b, c)$ can be obtained by

$$\hat{A}_{pk} = 2|a_{pk}|, \text{ and } \hat{\theta}_{pk} = \angle a_{pk}. \tag{13}$$

The amplitude and initial phase angle, as estimated by (13), can be used to update the ACT matrix $\mathbf{G}$ in (2) and also the complex amplitudes C_k and C_{-k} in (5). The above refinement algorithm can be iterated Q times until the estimated frequency converges to the actual value, where Q (≥ 2) is an integer. After all the iterations, the actual fundamental frequency can be achieved by $f_s\hat{f}$, where f_s is the sampling frequency. The proposed ACT-HAM method is presented in Table I.

III. Simulation Results

The performance of the ACT-HAM method is evaluated in MATLAB for different operating conditions of the grid voltages and is compared with other competing state-of-the art estimators. The system frequency is taken to be 50 Hz and the sampling frequency is chosen to be 4 kHz as this sampling frequency is common to many practical inverter systems. The Australian Power Standard AS/NZS 61000.2.2 outlines maximum allowable harmonic amplitudes for the distribution grid. This has been used to set the amplitudes of harmonics relative to the fundamental for this paper to emulate the worst-case harmonic distortion scenario as shown in Table II [22]. The fundamental voltage waveform parameters are given in Table III for the balanced and unbalanced cases [23]. In all of the results presented, the fundamental frequency is randomly varied in a range of 48-52 Hz, and the root mean squared error (RMSE) is obtained from 5000 Monte Carlo runs.

TABLE II: Harmonics Order and Corresponding Amplitudes

Harmonics	1^{st}	5^{th}	7^{th}	11^{th}
Amplitude	100%	6%	5%	3.2%

TABLE III: Fundamental Amplitudes and Initial Phase Angles

Balanced Parameters	Unbalanced Parameters
$A_a = A_b = A_c = 1.0$, $\theta_a = 10°$, $\theta_b = -110°$, $\theta_c = 130°$	$A_a = 0.8$, $A_b = 0.9$, $A_c = 1.0$, $\theta_a = 10°$, $\theta_b = -60°$, $\theta_c = 60°$

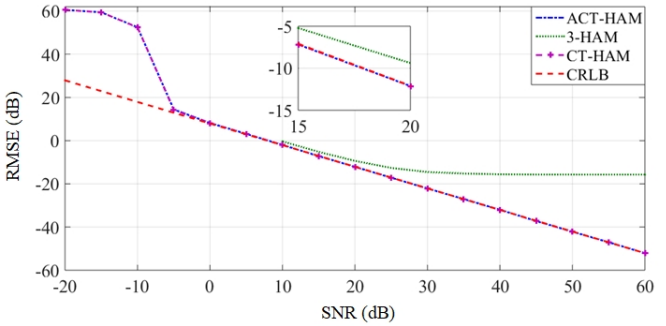

Fig. 1: RMSE of the fundamental frequency estimates versus SNR under harmonics and balanced condition when $N = 64$.

Fig. 1 compares the performance of the ACT-HAM, 3-HAM [23] and CT-HAM [24][25] estimators under balanced grid voltage conditions with harmonics from Table II for the following tuning condition: N=64 (80% of the nominal fundamental cycle) and Q=6. For this case, the SNR is varied in steps of 5 dB. It can be seen that both the adaptive and standard CT-based HAM estimators exhibit similar performances and converge to the CRLB. In this case, their SNR thresholds are -5 dB. On the other hand, the single-phase-based 3-HAM method fails when the SNR level is below 10 dB and cannot follow the CRLB when the SNR is more than 20 dB.

The noise performance comparison between the ACT-HAM, 3-HAM and CT-HAM methods for unbalanced grid voltage conditions including harmonics from Table II is presented in Fig. 2. For this result, the same tuning parameters, as the balanced case, are used for all the techniques. In addition, the performance of the 3-HAM estimator is evaluated for a higher number of iterations (Q=10 and 20). Similar to the balanced case, the SNR threshold of the 3-HAM estimator is 10 dB. On the other hand, the SNR threshold of both the ACT-HAM and CT-HAM methods is 0 dB, which is 5 dB higher than the balanced case. It can also be observed from Fig. 2 that, unlike the CT-HAM method, the ACT-HAM technique can converge to the CRLB under the unbalanced condition. After the SNR threshold, the RMSE of the CT-HAM method is around 5 dB

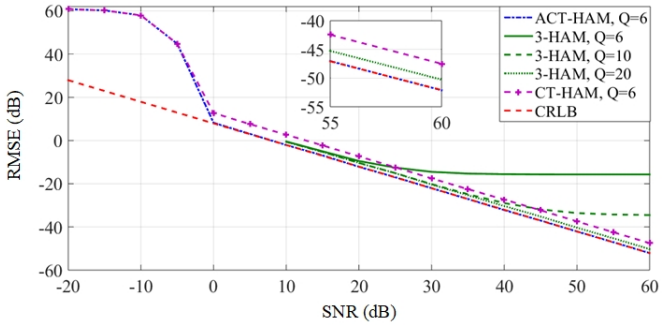

Fig. 2: RMSE of the fundamental frequency estimates versus SNR under harmonics and unbalanced condition when N = 64.

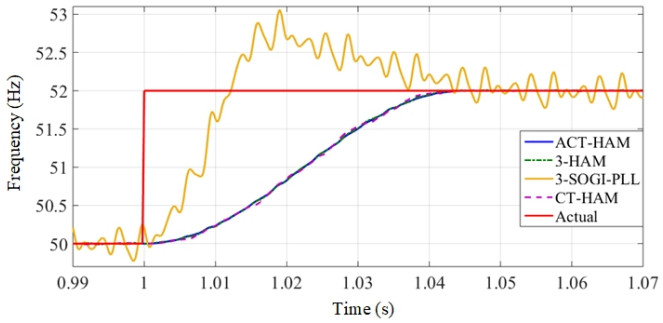

Fig. 3: Frequency estimation performance when the fundamental frequency experiences +2Hz step changes under harmonics and unbalanced condition.

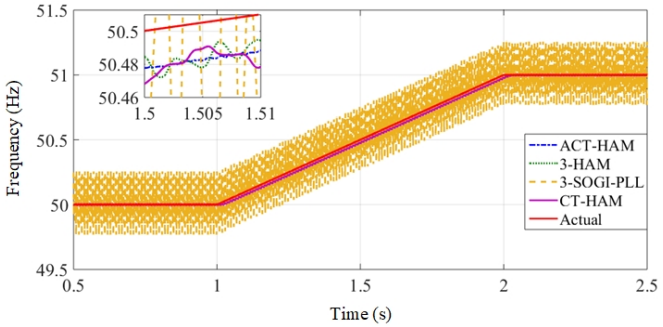

Fig. 4: Frequency estimation performance when the fundamental frequency experiences +1 Hz/s ramp changes under harmonics and unbalanced condition.

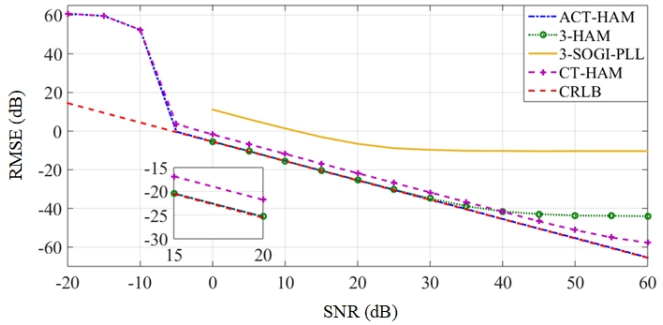

Fig. 5: RMSE of the fundamental frequency estimates versus SNR under harmonics and unbalanced condition when N = 180.

higher than the CRLB. On the other hand, the 3-HAM method can also follow the CRLB with a difference of around 2 dB, but it requires a higher number of iterations, such as Q=20, when compared to both CT-based methods.

The estimation of a step change of +2 Hz in the fundamental frequency during unbalanced grid voltage conditions with harmonics from Table II is demonstrated in Fig. 3. For this result comparison, the 3-SOGI-PLL method is tuned (SOGI's gain=2.1, proportional controller gain=137.5, integral controller gain=137.5^2/2.4, response time=45ms) according to [26] and a third-order discrete integrator, which generates better accuracy compared to the lower order integrator, is used for discrete implementation [27]. The ACT-HAM, CT-HAM and 3-HAM methods are also tuned (N=180: 225% of the nominal fundamental cycle, Q=3) to generate a similar response time (45 ms) during the frequency step condition. A sliding window approach is used for the HAM-based estimators and the estimation is updated when a new voltage sample is acquired. It can be noticed from Fig. 3 that the 3-SOGI-PLL produces large ripples at steady-state compared to the HAM-based methods for the same response time condition.

Results for when the fundamental frequency undergoes a ramp change under unbalanced conditions are shown in Fig. 4. The rate-of-change-of-frequency (RoCoF) of the fundamental frequency ramp is +1 Hz/s. It can be seen from Fig. 4 that all the four methods can track the frequency ramp, but the proposed ACT-HAM method creates less ripples during the change of the frequency.

The performance comparison of the HAM-based estimators with the 3-SOGI-PLL method under unbalanced conditions is presented in Fig. 5. The tuning parameters are the same as those used for the frequency step and ramp results shown above. Fig. 5 shows that the SNR thresholds of the ACT and CT-based HAM methods are improved by 5 dB for N=180 when compared to the case for N=64 shown in Fig. 2. Also, like the 3-HAM method, the 3-SOGI-PLL does not converge when the SNR is below 0 dB. However, unlike both the CT-HAM and 3-SOGI-PLL, the performance of the 3-HAM method is very close to the CRLB for the SNR range of 0-30 dB. The SNR threshold of the 3-HAM method is also enhanced by 10 dB when the window size is increased from N=64 to 180 samples, as can be observed from Figs. 2 and 5.

IV. Conclusions

A robust method relying on an adaptive Clarke transform and harmonic version of the Aboutanios and Mulgrew algorithm has been reported in this paper for tracking the three-phase grid frequency in the presence of harmonics, noise and imbalances. The proposed method mainly relies on spectral leakage free Fourier coefficients, which are adjacent to the maximum magnitude component in the spectrum, and an interpolation-based iterative approach for tracking the fundamental frequency. It has the ability to generate accurate frequency estimation and can also achieve the Cramèr Rao Lower Bound under both the balanced and unbalanced grid voltage conditions.

References

[1] M. R. Vedady Moghadam, R. T. B. Ma, and R. Zhang, "Distributed frequency control in smart grids via randomized demand response," *IEEE Trans. Smart Grid*, vol. 5, no. 6, pp. 2798–2809, 2014.

[2] W. Liu, G. Geng, Q. Jiang, H. Fan, and J. Yu, "Model-free fast frequency control support with energy storage system," *IEEE Trans. Power Syst.*, vol. 35, no. 4, pp. 3078–3086, 2020.

[3] "European standard en 50160 - voltage characteristics in public distribution systems," 2004.

[4] Y.-K. Wu, S.-M. Chang, and P. Mandal, "Grid-connected wind power plants: A survey on the integration requirements in modern grid codes," *IEEE Trans. Ind Appl.*, vol. 55, no. 6, pp. 5584–5593, 2019.

[5] P. Dash, A. Pradhan, and G. Panda, "Frequency estimation of distorted power system signals using extended complex kalman filter," *IEEE Trans. Power Del.*, vol. 14, no. 3, pp. 761–766, 1999.

[6] S. Golestan, M. Monfared, and F. D. Freijedo, "Design-oriented study of advanced synchronous reference frame phase-locked loops," *IEEE Trans. Power Electron.*, vol. 28, no. 2, pp. 765–778, 2013.

[7] X. He, H. Geng, and G. Yang, "A generalized design framework of notch filter based frequency-locked loop for three-phase grid voltage," *IEEE Trans. Ind. Electron.*, vol. 65, no. 9, pp. 7072–7084, 2018.

[8] Y. Xia and D. Mandic, "Widely linear adaptive frequency estimation of unbalanced three-phase power systems," *IEEE Trans. Instrum. Meas.*, vol. 61, no. 1, pp. 74–83, 2012.

[9] M. S. Reza, M. M. Hossain, and M. Ciobotaru, "Teager energy operator for fast estimation of three-phase grid frequency," *IEEE Trans. Instrum. Meas.*, vol. 70, pp. 1–10, 2021.

[10] M. S. Reza and M. M. Hossain, "Nonrecursive true open-loop approach for robust estimation of three-phase grid frequency," *IEEE Trans. Instrum. Meas.*, vol. 70, pp. 1–11, 2021.

[11] E. Aboutanios, "An adaptive clarke transform based estimator for the frequency of balanced and unbalanced three-phase power systems," in *2017 25th European Signal Process. Conf. (EUSIPCO)*, 2017, pp. 1001–1005.

[12] Y. Xia, L. Qiao, Q. Yang, W. Pei, and D. P. Mandic, "Widely linear adaptive frequency estimation for unbalanced three-phase power systems with multiple noisy measurements," in *2017 22nd International Conference on Digital Signal Processing (DSP)*, 2017, pp. 1–5.

[13] S. Kanna and D. Mandic, "Self-stabilising adaptive three-phase transforms via widely linear modelling," *Electronics Letters*, vol. 53, no. 13, pp. 875–877, 2017.

[14] D. P. Mandic, S. Kanna, Y. Xia, A. Moniri, A. Junyent-Ferre, and A. G. Constantinides, "A data analytics perspective of power grid analysis-part 1: The clarke and related transforms," *IEEE Signal Process. Mag.*, vol. 36, no. 2, pp. 110–116, 2019.

[15] R. Schmidt, "Multiple emitter location and signal parameter estimation," *IEEE Trans. Antennas Propag.*, vol. 34, no. 3, pp. 276–280, 1986.

[16] R. Roy and T. Kailath, "ESPRIT-estimation of signal parameters via rotational invariance techniques," *IEEE Trans. Acoustics, Speech and Signal Process.*, vol. 37, no. 7, pp. 984–995, 1989.

[17] S. Ye and E. Aboutanios, "An algorithm for the parameter estimation of multiple superimposed exponentials in noise," in *2015 IEEE International Conf. Acoustics, Speech and Signal Proc. (ICASSP)*, 2015, pp. 3457–3461.

[18] ——, "Iterative windowed parameter estimation of multiple superimposed damped exponentials in noise," in *2015 23rd European Signal Process. Conf. (EUSIPCO)*, 2015, pp. 2201–2205.

[19] E. Aboutanios and B. Mulgrew, "Iterative frequency estimation by interpolation on fourier coefficients," *IEEE Trans. Signal Process.*, vol. 53, no. 4, pp. 1237–1242, 2005.

[20] Z. Chen, Z. Sahinoglu, and H. Li, "Fast frequency and phase estimation in three phase power systems," in *2013 IEEE PES General Meet.* IEEE, 2013, pp. 1–5.

[21] J. Sun, E. Aboutanios, and D. B. Smith, "Iterative weighted least squares frequency estimation for harmonic sinusoidal signal in power systems," in *2018 26th European Signal Process. Conf. (EUSIPCO)*, 2018, pp. 176–180.

[22] "As/nzs standard 61000.2.2, "electromagnetic compatibiity (emc) environment - compability levels for low-frequency conducted disturbances and signalling in public low-voltage power supply systems," 2003.

[23] J. Sun, E. Aboutanios, and D. B. Smith, "Low cost and precise frequency estimation in unbalanced three phase power systems," *IEEE Trans. Power Del.*, pp. 1–10, 2022.

[24] J. Sun, E. Aboutanios, D. B. Smith, and J. E. Fletcher, "Robust frequency, phase, and amplitude estimation in power systems considering harmonics," *IEEE Trans. Power Del.*, vol. 35, no. 3, pp. 1158–1168, 2020.

[25] J. Sun, S. Ye, and E. Aboutanios, "Robust and rapid estimation of the parameters of harmonic signals in three phase power systems," in *2016 24th European Signal Process. Conf. (EUSIPCO)*, 2016, pp. 408–412.

[26] S. Golestan, M. Monfared, F. D. Freijedo, and J. M. Guerrero, "Dynamics assessment of advanced single-phase pll structures," *IEEE Trans. Ind. Electron.*, vol. 60, no. 6, pp. 2167–2177, 2013.

[27] M. Ciobotaru, R. Teodorescu, and F. Blaabjerg, "A new single-phase pll structure based on second order generalized integrator," in *2006 37th IEEE Power Electron. Specialists Conf.*, 2006, pp. 1–6.